

Microstrip Open-Slot Antenna with Wideband Dual-Frequency and Dual-Sense Circular Polarization

Tingting Chen*, Jingjing Zhang, and Lu Hua

Abstract—A wideband microstrip open-slot antenna with dual-frequency dual-sense circular polarization (CP) is presented in this paper. A bent feeding structure and three radiating slots, including a modified cross-shaped, an inverted F-shaped, and an inverted L-shaped slots, are designed to excite two orthogonal electric fields with a quadrature phase difference for a radiating right-hand circularly polarized (RHCP) wave at 2.5 GHz and left-hand circularly polarized (LHCP) wave at 3.3 GHz. To improve the axial-ratio (AR), a bent parasitic element is introduced near the microstrip line. Multiple resonances are merged to achieve a large bandwidth of 2620 MHz (104.8%) from 2.2 GHz to 4.82 GHz. The measured AR bandwidths are 460 MHz (18.4%) at the lower band (2.5 GHz) and 2150 MHz (65.1%) at the upper band (3.3 GHz).

1. INTRODUCTION

Recently, with the development of modern wireless communication, dual-frequency circularly polarized antennas have attracted much attention due to high polarization efficiency. Circularly polarized waves are powerful in satellite communications and global positioning systems, since circularly polarized waves will not be rotated like the linear polarized waves when they pass through ionosphere [1, 2]. The injected power of slot antennas is transmitted to the radiation aperture through electromagnetic coupling, and the antennas have the advantages of low profile, simple structure, and wide bandwidth [3–5]. Slots with different shapes are etched on the conductive grounding plane of the slot antenna to excite required resonant modes and radiate power into free space. Compared with traditional half-wavelength closed slot antenna, the length of the open slot antenna is usually about a quarter of the wavelength [6], which makes the size of the open slot antenna more compact. Printed slot antenna is an inherently linearly polarized radiator [7], so exciting two orthogonal resonant modes to produce CP waves is a challenging research topic. Several types of circularly polarized open slot antennas have been proposed [8–10], recently. In [8], an L-shaped slot circularly polarized antenna fed by a bent microstrip line is proposed, which achieves an axial ratio of 23% at 1.6 GHz. By introducing an asymmetrically disturbed open slot and a wide tuning stub at the lower left of the slot, a coplanar waveguide antenna with a 27% axial ratio bandwidth operating at 3.7 GHz is formed [9]. A coplanar waveguide-fed open cross-slot antenna is developed in [10], and 48% wide impedance bandwidth and 8.9% axial ratio bandwidth are obtained. Dual-frequency dual-sense CP is beneficial to the alleviation of multipath interference and fading effects [11–13]. A dual-frequency dual-sense circularly polarized antenna realized by designing an F-shaped feeding structure and parasitic elements is presented to achieve AR bandwidths of 22.22% at 1.8 GHz and 10.53% at 3.3 GHz, respectively [14].

In this communication, a dual-frequency dual-sense circularly polarized open-slot antenna with broadband CP and wide impedance bandwidth is presented. By locating the open cross slot optimally

Received 27 May 2019, Accepted 26 July 2019, Scheduled 5 August 2019

* Corresponding author: Tingting Chen (ctt.ting@126.com).

The authors are with the College of Electronic Information Engineering, Shandong University of Science and Technology, Qingdao, Shandong 266590, China.

on the edge of the ground plane, the antenna is able to not only possess a good impedance bandwidth, but also generate a CP wave at 2.5 GHz. Due to the addition of the inverted F-shaped slot and L-shaped slot, dual-frequency dual-sense CP is achieved. Moreover, a bent parasitic element is added near the feeding line to improve the CP performance at the higher frequency (3.3 GHz) band. The proposed antenna can be used for WLAN and WiMAX band with CP characteristics.

2. ANTENNA CONFIGURATION

Figure 1 shows the configuration of the proposed open-slot antenna. The antenna is fabricated on an FR4 microwave substrate with a thickness of 1.6 mm, relative dielectric constant of 4.4, and tangent loss of 0.02. In this design, the slot structure of the antenna consists of a modified unequal cross slot, an inverted L-shaped slot at the left edge of the ground plane, and an inverted F-shaped slot rotated 90° anti-clockwise and connected to the right arm of the cross slot. A bent feeding structure [15] is used as

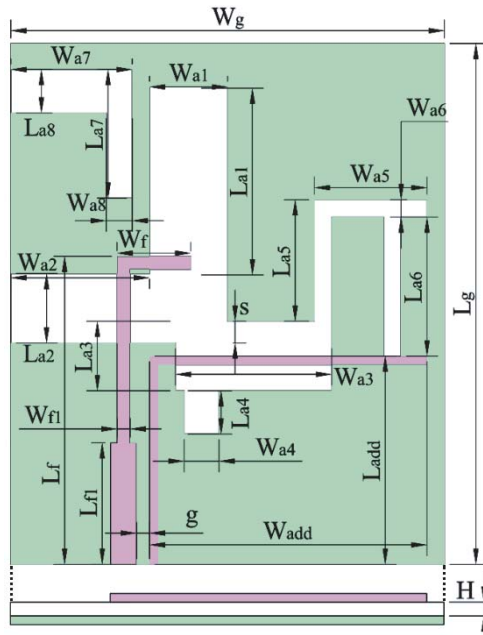


Figure 1. Configuration of the proposed open-slot antenna.

Table 1. Geometrical parameters of the proposed antenna (unit: mm).

Parameter	Value	Parameter	Value	Parameter	Value
W_g	50	W_{a5}	13	L_{a8}	5
L_g	60	L_{a5}	14	W_{f1}	1.5
W_{a1}	9	W_g	50	L_{f1}	14
L_{a1}	21.5	L_g	60	W_f	8.5
W_{a2}	16	W_{a6}	2	L_f	35.5
L_{a2}	8	L_{a6}	16	W_{add}	32
W_{a3}	18	W_{a7}	14	L_{add}	24
L_{a3}	8	L_{a7}	14.8	W_{a6}	2
W_{a4}	4	W_{a8}	3	L_{a6}	16
L_{a4}	5				

a power injection element for the improvement of impedance matching and CP performance. A series of adjustments, such as the evolution from L-shaped slot to cross-shaped slot and the modification of the cross-shaped slot, not only increase the impedance bandwidth of the antenna, but also lead to the generation of high-frequency CP wave. The utilization of the inverted F-shaped slot and L-shaped slot improves the CP performance at high frequencies and the impedance matching at low frequencies, respectively. Finally, a bent parasitic element is introduced near the feeding structure, and the coupling between them affects the magnetic fields of the cross slot and inverted F-shaped slot, which greatly improves the CP bandwidth and excites an additional resonance at 6.18 GHz. Table 1 lists the dimensional parameters of the proposed antenna after the optimization.

3. ANTENNA DESIGN AND ANALYSIS

The initial design process of the dual-frequency dual-sense CP antenna can be illustrated by the improvement of the three antenna prototypes in Figure 2. Ant.1 shown in Figure 2(a) is the prototype of the antenna, which is modified according to the design in [13]. Ant.1 is an open slot antenna with a bent feeding structure and an inverted L-shaped slot on the left side of the ground plane. The curvature of the upper end of the microstrip feed line increases the current density at the upper end of the slot and produces a CP wave at 3 GHz. When the upper end (L_{a1}) of the L-shaped slot extends to 21.5 mm, and an L-shaped slot in the opposite direction is added to the lower end to construct a cross slot, the antenna exhibits a dual-frequency mechanism with a bandwidth ranging from 2.2 GHz to 4.7 GHz. In order to excite the frequency about 4 GHz, the size of the slot can be roughly determined by the following formula [16]:

$$f = \frac{c}{2w\sqrt{\epsilon_{re}}} \quad (1)$$

where c is the speed of light in the air, ϵ_{re} the effective dielectric constant, and w the length of the slot. Accordingly, the initial slot length W_{a3} in this design is approximately 17.8 mm. The lower frequency resonance shifts down while a resonance at the higher frequency is also excited. Ant.3 mainly improves the dislocation of the lower end of the cross slot and adopts a step structure to upgrade the coupling between the slot and feed line, resulting in a wideband response [17]. For a comprehensive comparison of the three antennas, Figure 3 shows the reflection coefficients and axis ratios obtained on the z -axis relative to the frequency changes. From the simulation results shown in Figure 3(b), it can be observed that the designs of extending the upper end of the slot and constructing the cross slot not only generate an additional resonance at 4.3 GHz, but also enlarge the bandwidth by merging the two resonances. As the amplitude difference between the horizontal current and vertical current decreases, the axial ratio at the higher frequency decreases. Although the cross slot of Ant.2 reduces the axial ratio of linear polarization in the entire frequency band, it eliminates the circular polarization in the lower band. Comparing Ant.2 and Ant.3, the modification of the cross slot and the design of the step structure allow the antenna to achieve the available circular polarization in the lower band of 2.4–2.6 GHz.

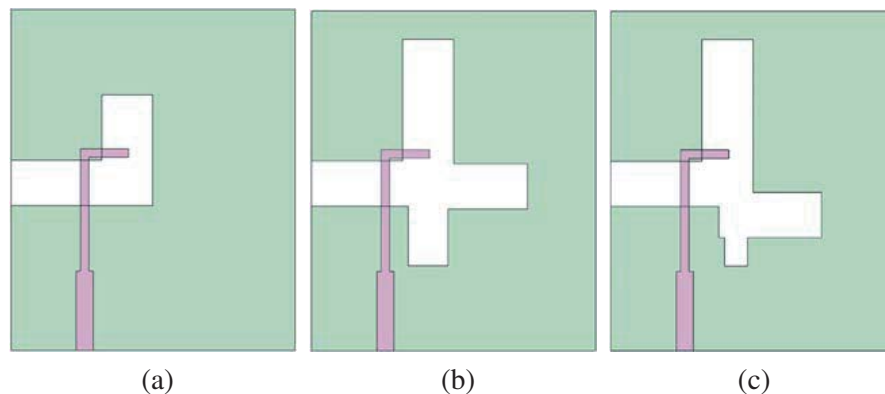


Figure 2. Three improved prototypes of the cross-shaped slot antenna. (a) Ant.1, (b) Ant.2, (c) Ant.3.

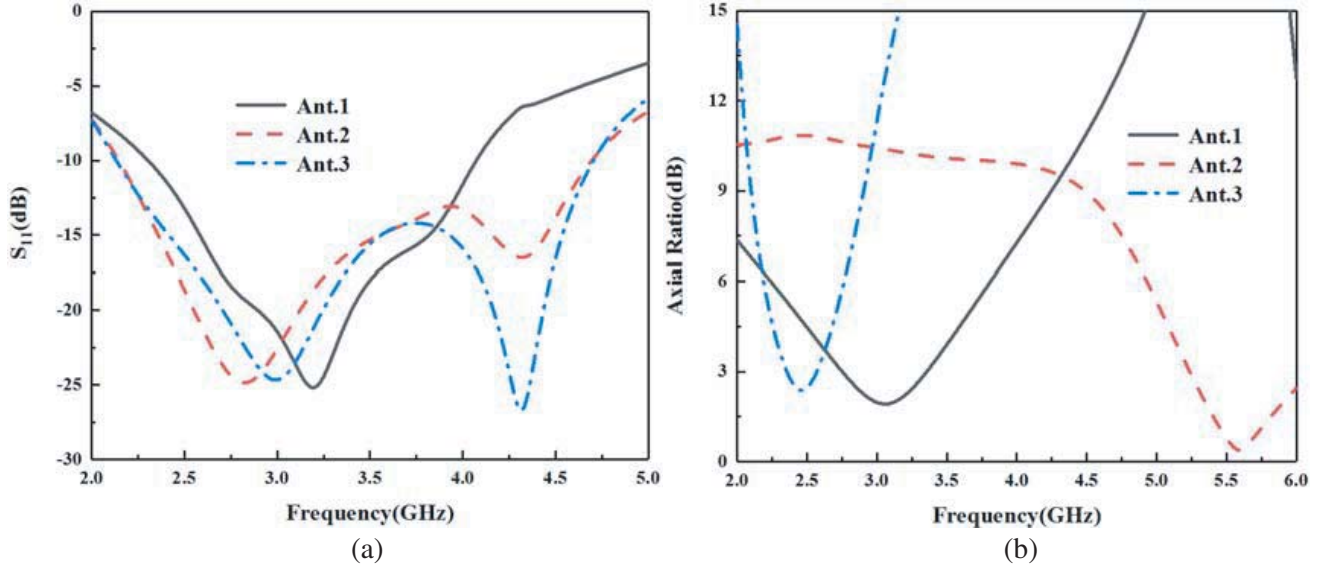


Figure 3. (a) Simulated S_{11} and (b) axial ratio of Ant.1–3.

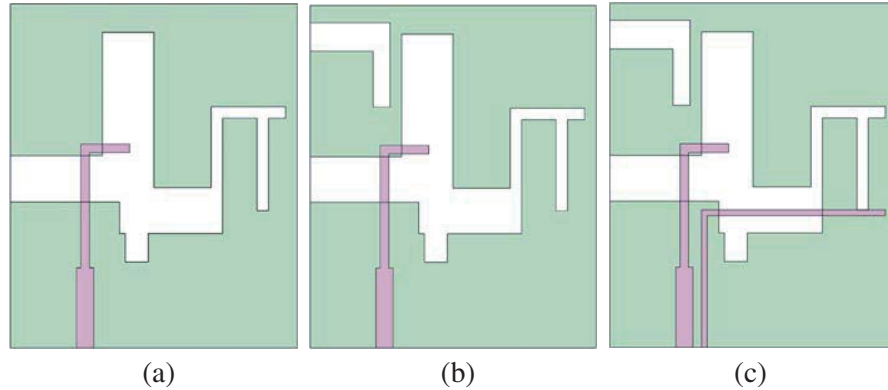


Figure 4. Three improved prototypes of the proposed antenna. (a) F-slot, (b) FL-slot, (c) proposed.

In Figures 4 and 5, the design evolution of the open slot antenna and its corresponding S_{11} and AR diagrams are shown. The antenna with an F-slot or an FL-slot is denoted by F-slot antenna or FL-slot antenna. An F-shaped slot which is rotated 90° anticlockwise is applied to the right side of the cross slot resulting in an additional resonance at about 3.5 GHz and a circular polarization at 5.8 GHz. As shown in Figure 4(b), an inverted L-shaped slot is embedded in the upper left side of the ground plane, which improves the impedance matching at lower frequencies. The utilization of the inverted L-shaped slot has a greater influence on the circular polarization at higher frequency, which greatly reduces the axial ratio, and the CP at the lower frequency is slightly shifted downward compared to the F-slot antenna. Figure 5 indicates the comparison of S_{11} and AR of the antenna with and without the bent parasitic element. After adding the parasitic element, the impedance matching at the lower and higher resonances is improved. It is worth noting that a new resonance is also produced at 5.8 GHz. The bent parasitic element mainly affects the magnetic field in the lower half of the cross slot and F-shaped slot, resulting in magnetic field disturbance in the slot [8], which greatly increases the circular polarization bandwidth at the high frequency of the antenna. The simulated AR bandwidths are 390 MHz and 2250 MHz, about 16% and 70%, respectively.

The magnetic current density distributions of the proposed antenna simulated by HFSS software at different frequencies are shown in Figure 6. For the 2.62 GHz-band excitation, the magnetic current

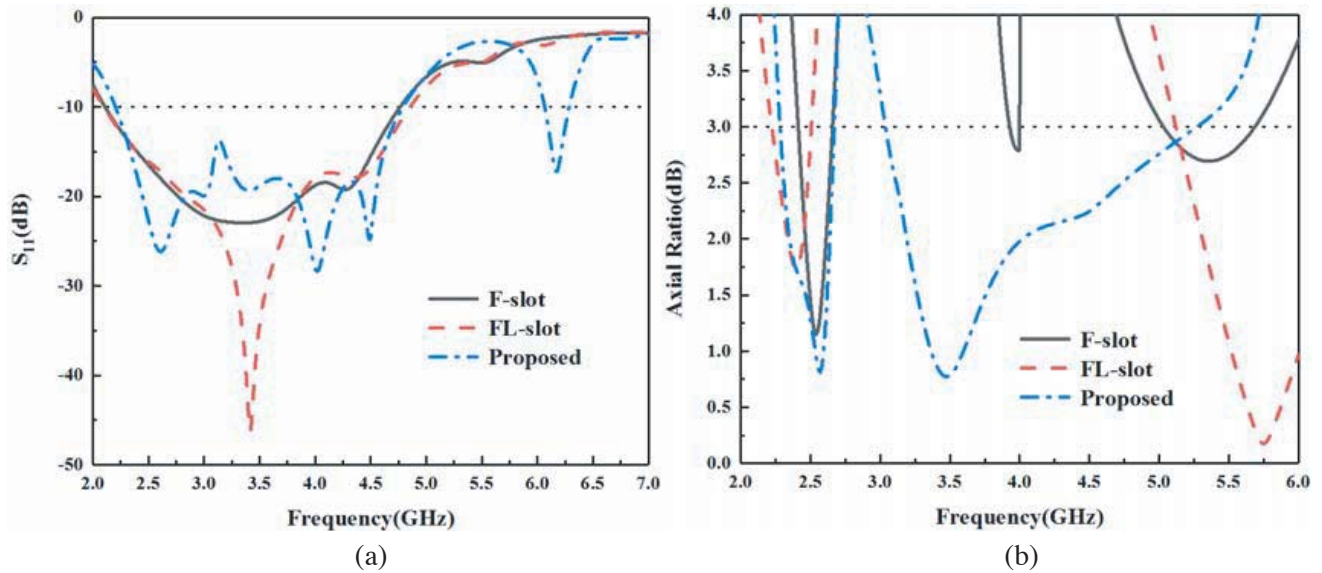


Figure 5. (a) Simulated S_{11} and (b) axial ratio of the three types of antennas.

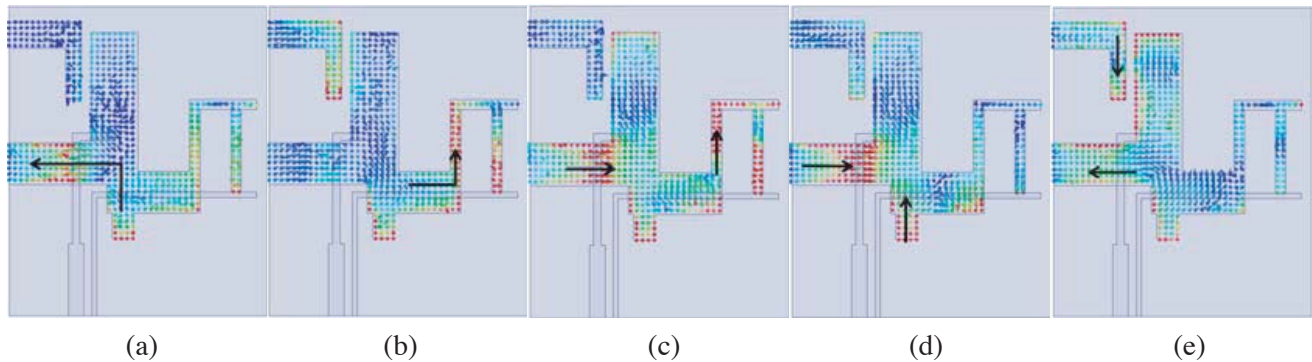


Figure 6. Distributions of magnetic current density of the proposed antenna. (a) 2.62 GHz, (b) 3 GHz, (c) 4.02 GHz, (d) 4.49 GHz, (e) 6.18 GHz.

paths consist of the cross arm portion of the cross slot and vertical portion of the F-shaped slot, whereas the 3 GHz current paths are the vertical portions of the L-shaped slot and F-shaped slot. The radiation patterns at 4.02 GHz and 4.49 GHz are influenced by the cross arm and lower arm of the cross slot and F-shaped slot. In Figure 6(e), the addition of the bent parasitic element contributes to the resonance of 6.18 GHz at high frequency, mainly affecting the magnetic fields of the lower arm and right arm of the cross slot and F-shaped slot. Furthermore, the magnetic current distribution at the interface between the inverted L-shaped slot and upper arm of the cross slot indicates that the injected power of the inverted L-shaped slot is coupled from the cross slot.

The simulated magnetic current distributions of the proposed open slot antenna varying with phase at 2.5 GHz and 3.3 GHz are shown in Figure 7 and Figure 8. It can be observed that the CP wave of 2.5 GHz is excited by the left arm and vertical portion of the cross slot where the magnetic current is concentrated, while the circular polarization of 3.3 GHz is excited from the right arm of the cross slot and F-shaped slot. From Figures 7(a)–(d), at 0° , the predominant magnetic currents are concentrated in the left arm and upper arm parts of the cross slot and are directed relative to the $-x$ axis and $+y$ axis, respectively. At a later time instant with a 90° phase lagging, the principal magnetic currents are along the left arm and lower arm of the cross slot, and face the directions with respect to the $+x$ axis and $-y$ axis, respectively. At 180° and 270° , the magnetic current distributions are just opposite to 0°

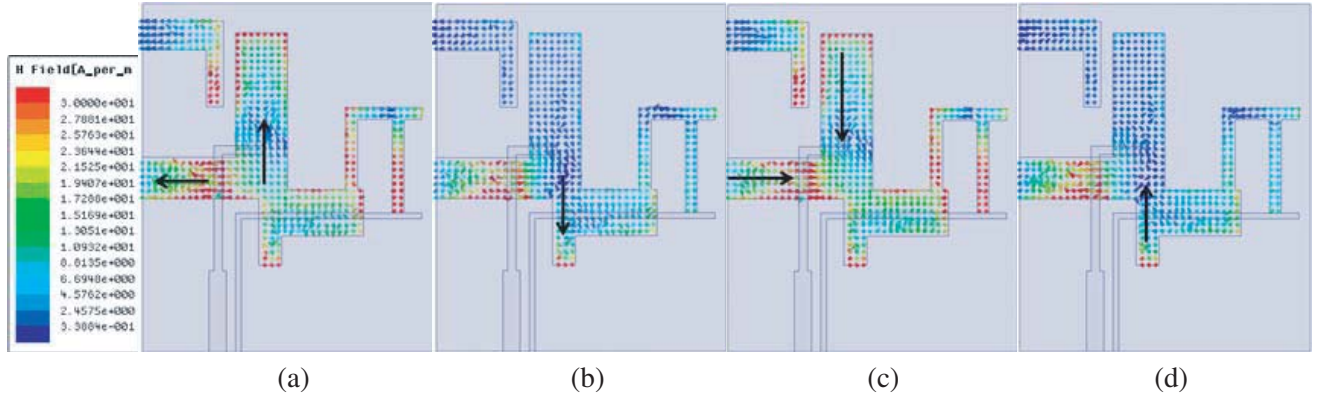


Figure 7. Simulated magnetic current distributions for the CP center frequency at 2.5 GHz. (a) 0° , (b) 90° , (c) 180° , (d) 270° .

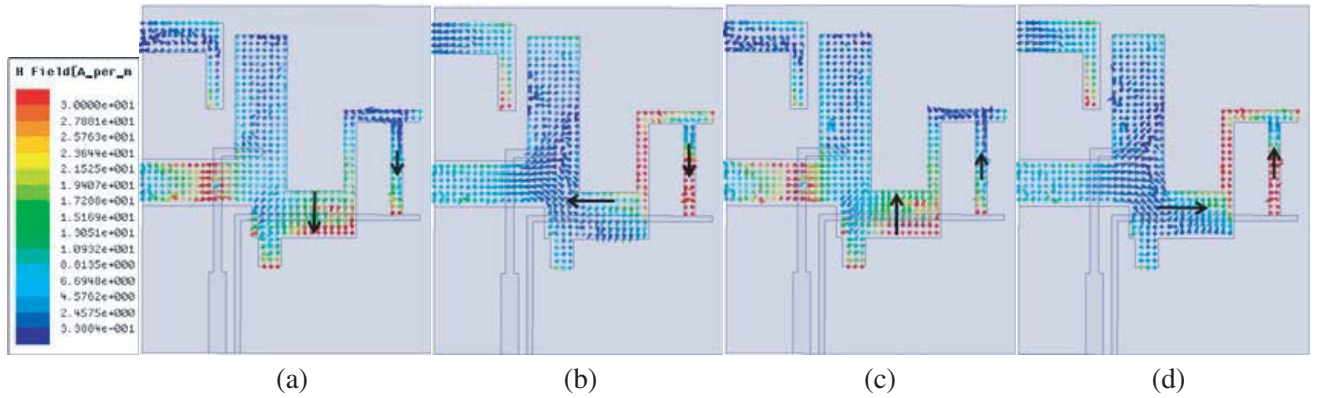


Figure 8. Simulated magnetic current distributions for the CP center frequency at 3.3 GHz. (a) 0° , (b) 90° , (c) 180° , (d) 270° .

and 90° , respectively. At 2.5 GHz, the currents rotate anticlockwise with phase to yield an RHCP wave in the bore-sight direction and at 3.3 GHz, rotate clockwise to generate an LHCP wave.

4. PARAMETRIC STUDY

Figure 9 shows the variations of S_{11} with frequency for various lengths (L_{add} and W_{add}) of the bent parasitic element. As shown in Figure 9(a), the increase in the parasitic element horizontal length (L_{add}) causes the resonance at the higher frequency to shift upward, and the impedance matching at the low frequency of 2.5 GHz and the intermediate frequency of 4 GHz is deteriorated. It can be found that compared with the vertical part length L_{add} of the bent parasitic element, the horizontal part length W_{add} has a greater influence on the reflection coefficient. As the length of W_{add} increases, that is, the parasitic unit is closer to the bent microstrip line, the impedance matching of other frequency bands becomes worse except for the high frequency of 6.18 GHz. Therefore, the placement position of the bent parasitic element has a great influence on the antenna performance. From Figure 10, it is noted that with the changes of W_{add} and L_{add} , the axial ratio at the low frequency of the antenna is substantially unaffected while the axial ratio at the high frequency varies relatively. This is because the parasitic element mainly affects the magnetic fields in the lower arm and right arm of the cross slot and inverted F-shaped slot which produce circular polarization at the higher frequency, without affecting the left arm and upper arm which generate circular polarization at the lower frequency.

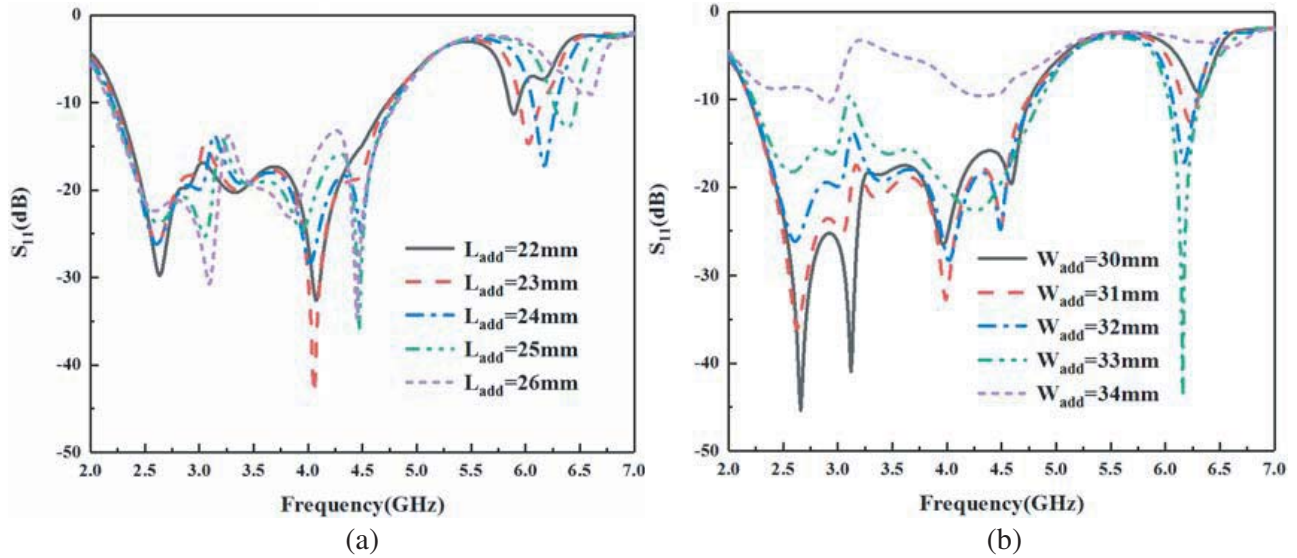


Figure 9. S_{11} with different values of (a) L_{add} and (b) W_{add} .

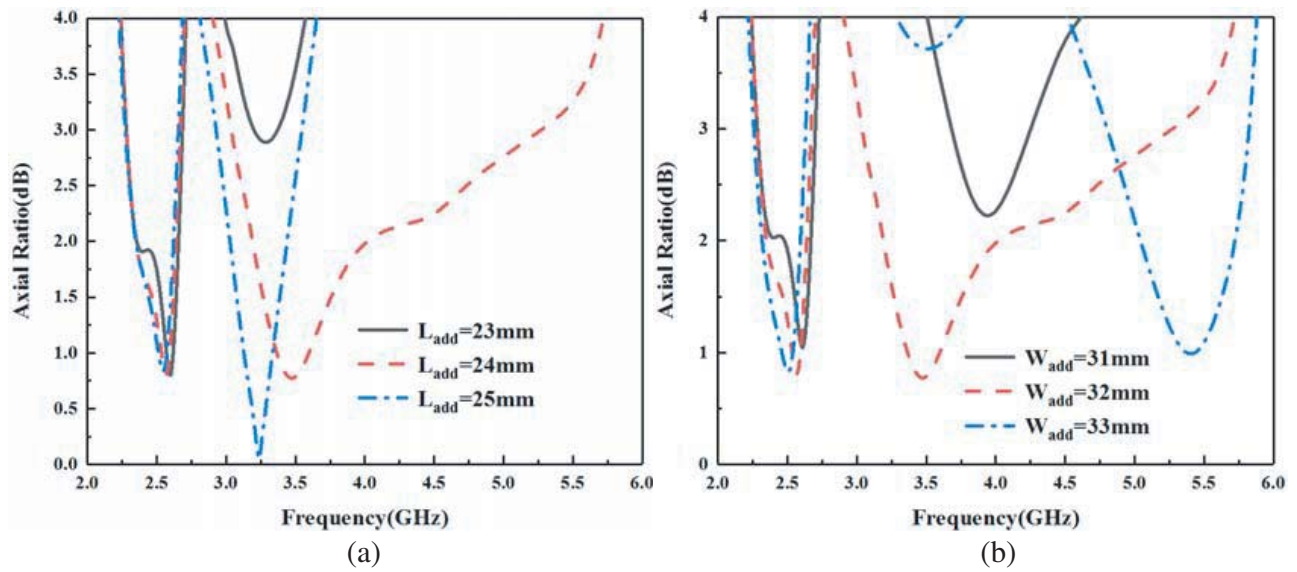


Figure 10. Axial ratio with different values of (a) L_{add} and (b) W_{add} .

5. RESULTS

To validate the proposed design, a prototype is fabricated, as shown in Figure 11. The measured impedance bandwidth with $S_{11} < -10$ dB is 104.8% from 2.2 GHz to 4.82 GHz, as shown in Figure 12. As shown in Figure 13, the measured 3 dB AR bandwidths of the antenna can reach 460 MHz at 2.5 GHz with a relative bandwidth of 18.4% and can reach 2150 MHz at 3.3 GHz with a relative bandwidth of 65.1%. The gains in measurement are 1.8–3.6 dBi. Figure 14 depicts the measured and simulated radiation patterns of RHCP and LHCP in the xz - and yz -plane, respectively, for 2.5 and 3.3 GHz. At 2.5 GHz, the antenna radiates a right-hand circularly polarized wave, and it can be observed that the level of cross-polarization in the maximum radiation direction ($+z$) is about ≥ 20 dB. The antenna radiates a left-handed circularly polarized wave at 3.3 GHz, and Figure 14(b) shows that the cross-polarization level of the antenna in the maximum radiation direction ($+z$) is approximately ≥ 18 dB.

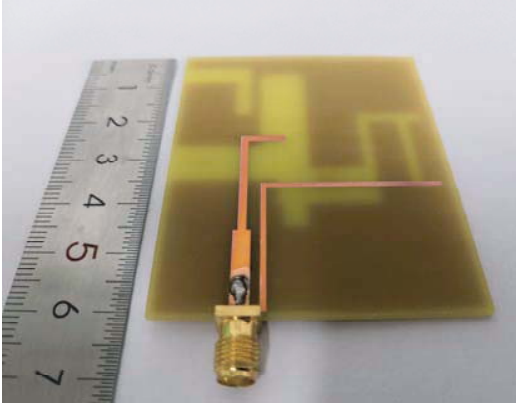


Figure 11. Photograph of proposed antenna.

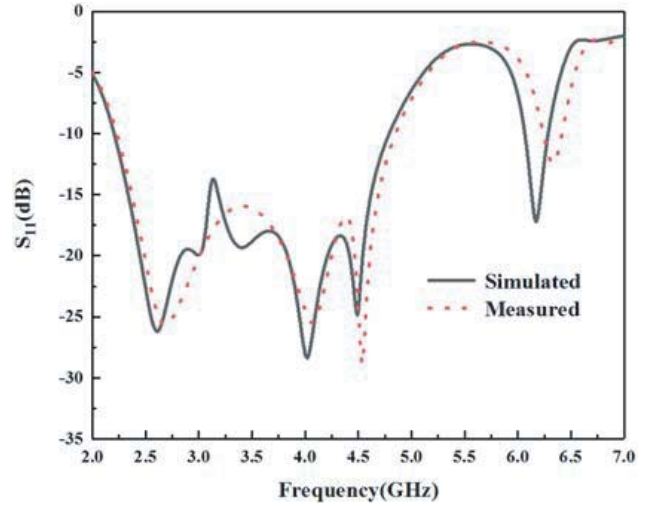


Figure 12. Simulated and measured S_{11} .

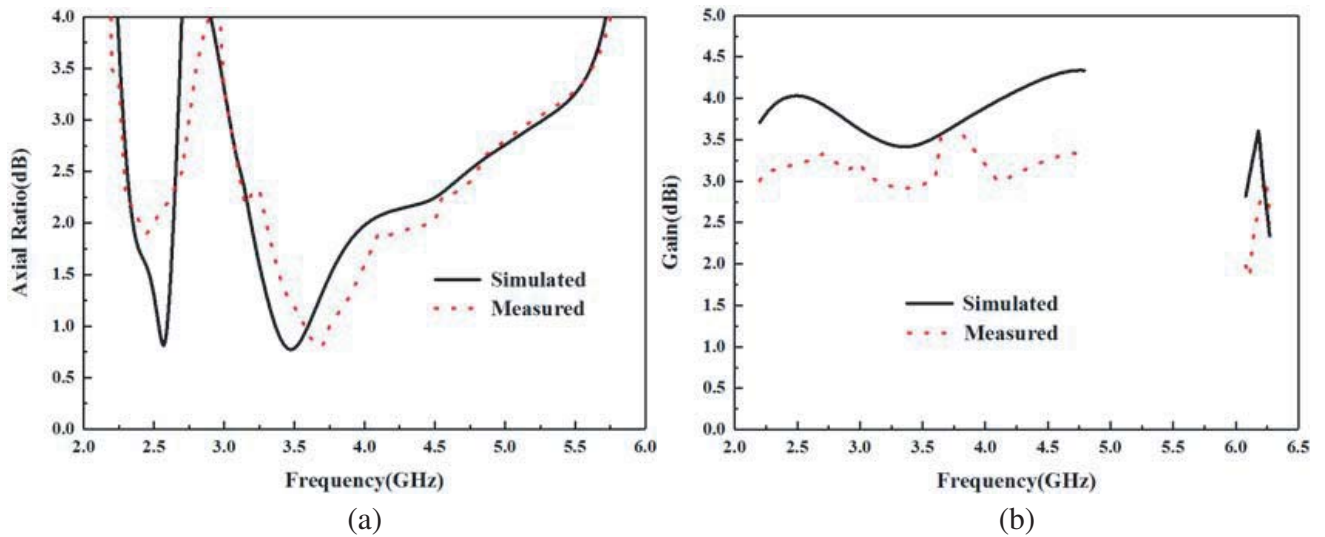


Figure 13. Simulated and measured axial ratio coefficients and gains of proposed antenna.

Table 2. Performance comparison between the proposed antenna and reported antennas.

	Size; mm ²	Freq.; GHz	Polarization	S_{11} BW%	AR BW%
Ref. [8]	70 × 70	1.68	RHCP	30	32
Ref. [9]	50 × 50	3.7	RHCP	111	27
Ref. [10]	50 × 60	2.24	LHCP	48.8	8.9
Ref. [11]	50 × 50	3.5/5.7	DUAL CP	91.85	13.56/8.17
Ref. [12]	70 × 70	1.7/2.55	DUAL CP	106.9	32.35/5.6
Ref. [13]	63 × 75	2.55/3.53	DUAL CP	71.63	27.45/7.1
Ref. [14]	63.5 × 55	1.8/3.325	DUAL CP	26.04/18.93	22.22/10.53
Proposed	60 × 70	2.5/3.3	DUAL CP	104.8	18.4/65.1

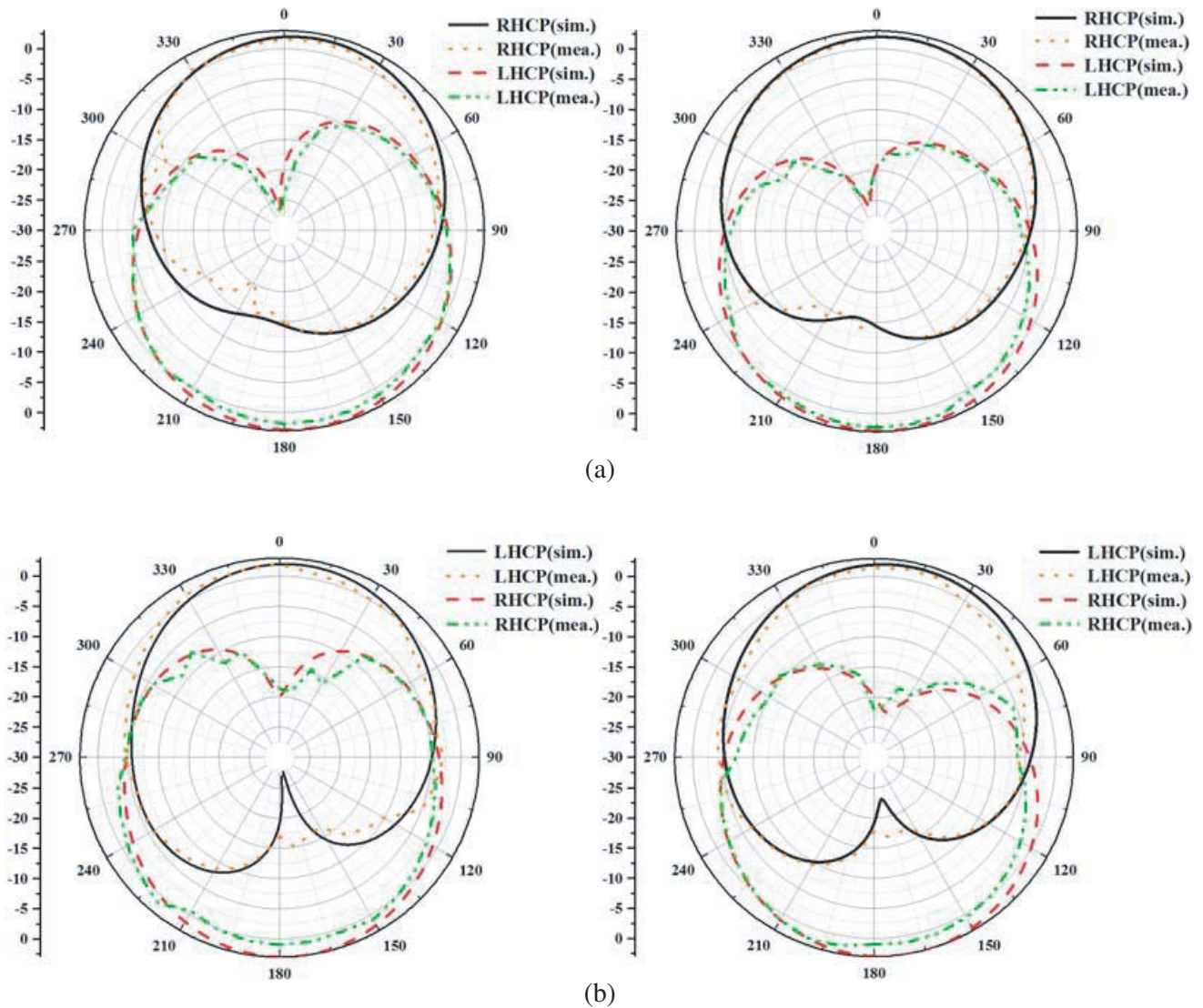


Figure 14. Simulated and measured radiation patterns at (a) 2.5 GHz and (b) 3.3 GHz.

The comparison between the measured performances of the proposed antenna and antennas reported in [8–14] is listed in Table 2, which includes antenna size, sense of polarization, IBW, and 3 dB ARBW. The proposed dual-frequency dual-sense circularly polarized antenna shows larger impedance and 3-dB AR bandwidths.

6. CONCLUSION

In this paper, a dual-frequency dual-sense circularly polarized slot antenna with wide impedance bandwidth and wide CP has been demonstrated. By introducing a bent parasitic element near the bent feeding structure, the CP bandwidth is enhanced. The antenna utilizes a bent feeding structure and three radiating slots, which can not only possess a wide impedance bandwidth, but also excite dual-frequency circularly polarized waves for RHCP at 2.5 GHz and for LHCP at 3.3 GHz. The measurement results show that the proposed antenna has the impedance bandwidth of 104.8% and 3 dB AR bandwidths of 18.4% and 65.1% for the two operating bands, respectively. The attractive performance of the proposed antenna makes it a candidate for multifunctional integration of wireless communication systems.

REFERENCES

1. Qin, Y., S. Gao, and A. Sambell, "Broadband high-efficiency circularly polarized active antenna and array for RF front-end application," *IEEE Transactions on Microwave Theory and Techniques*, Vol. 54, 2910–2916, 2006.
2. Qin, Y., S. Gao, and A. Sambell, "Broadband high-efficiency linearly and circularly polarized active integrated antennas," *IEEE Transactions on Microwave Theory and Techniques*, Vol. 54, 2723–2732, 2006.
3. Heydari, S., P. Jahangiri, A. S. Arezoomand, and F. B. Zarrabi, "Circular polarization fractal slot by jerusalem cross slot for wireless applications," *Progress In Electromagnetics Research Letters*, Vol. 63, 79–84, 2016.
4. Chen, C., X. Zhang, S. Qi, and W. Wu, "Wideband circular polarization cavity-backed slot antenna for GNSS applications," *Progress In Electromagnetics Research Letters*, Vol. 52, 31–36, 2015.
5. Huang, H.-F. and B. Wang, "A simple V-shaped slot antenna with broadband circular polarization," *Progress In Electromagnetics Research Letters*, Vol. 67, 67–73, 2017.
6. Zhao, A. P. and J. Rahola, "Quarter-wavelength wideband slot antenna for 3–5 GHz mobile applications," *IEEE Antennas and Wireless Propagation Letters*, Vol. 4, 421–424, 2005.
7. Wong, K.-L., J.-Y. Wu, and C.-K. Wu, "A circularly polarized patch-loaded square-slot antenna," *Microwave and Optical Technology Letters*, Vol. 23, 363–365, 2015.
8. Mousavi, P., B. Miners, and O. Basir, "Wideband L-shaped circular polarized monopole slot antenna," *IEEE Antennas and Wireless Propagation Letters*, Vol. 9, 822–825, 2010.
9. Jan, J.-Y., C.-Y. Pan, K.-Y. Chiu, and H.-M. Chen, "Broadband CPW-fed circularly-polarized slot antenna with an open slot," *IEEE Transactions on Antennas and Propagation*, Vol. 61, 1418–1422, 2013.
10. Wang, C.-J. and C.-M. Lin, "A CPW-fed open-slot antenna for multiple wireless communication systems," *IEEE Antennas and Wireless Propagation Letters*, Vol. 11, 620–623, 2012.
11. Midya, M., S. Bhattacharjee, and M. Mitra, "CPW-fed dual-band dual-sense circularly polarized antenna for WiMAX application," *Progress In Electromagnetics Research Letters*, Vol. 81, 113–120, 2019.
12. Chen, Y.-Y., Y.-C. Jiao, G. Zhao, F. Zhang, Z.-L. Liao, and Y. Tian, "Dual-band dual-sense circularly polarized slot antenna with a C-shaped grounded strip," *IEEE Antennas and Wireless Propagation Letters*, Vol. 10, 915–918, 2011.
13. Saini, R. K., S. Dwari, and M. K. Mandal, "CPW-fed dual-band dual-sense circularly polarized monopole antenna," *IEEE Antennas and Wireless Propagation Letters*, Vol. 16, 2497–2500, 2017.
14. Saini, R. K. and P. S. Bakariya, "Dual-band dual-sense circularly polarized asymmetric slot antenna with F-shaped feed line and parasitic elements," *Progress In Electromagnetics Research M*, Vol. 69, 185–195, 2018.
15. Steven Yang, S.-L., A. A. Kishk, and K.-F. Lee, "Wideband circularly polarized antenna with L-shaped slot," *IEEE Transactions on Antennas and Propagation*, Vol. 56, 1780–1783, 2012.
16. Chen, W.-L., G.-M. Wang, and C.-X. Zhang, "Bandwidth enhancement of a microstrip lined printed wide-slot antenna with a fractal-shaped slot," *IEEE Transactions on Antennas and Propagation*, Vol. 60, 1712–1716, 2012.
17. Purohit, P., B. K. Shukla, and D. K. Raghuvanshi, "An investigation of stepped open slot antenna with circular tuning stub," *Progress In Electromagnetics Research C*, Vol. 91, 157–171, 2019.